Zero-dimensional Nonlinear Burn Control Using Isotopic Fuel Tailoring For Thermal Excursions

Mark D. Boyer and Eugenio Schuster

***Abstract*— The control of plasma density and temperature are among the most fundamental problems in fusion reactors and will be critical to the success of burning plasma experiments like ITER. While stable burn conditions exist, it is possible that economic and technological constraints will require future commercial reactors to operate with low temperature, high density plasma, a burn condition that may be unstable. The instability is due to the fact that for low temperatures, the fusion heating increases as the plasma temperature rises. An active control system will be essential for stabilizing such operating points. In this work a spatially averaged (zero-dimensional) nonlinear transport model for the energy and the densities of deuterium and tritium fuel ions, as well as the alpha-particles, is used to synthesize a nonlinear feedback controller for stabilizing the burn condition of a fusion reactor. Whereas previous efforts assume an optimal 50:50 mix of deuterium and tritium fuel, this controller makes use of ITER's planned isotopic fueling capability and controls the densities of these ions separately. Also, unlike previous work which used impurity injection to mitigate thermal excursions, this design exploits the ability to modulate the DT fuel mix to control the plasma heating. By moving the isotopic mix in the plasma away from the optimal 50:50 mix, the reaction rate is slowed and the alpha-particle heating is reduced to desired levels. A zero-dimensional simulation study is presented to show the ability of the controller to bring the system back to the desired equilibrium from a given set of perturbations.**

I. INTRODUCTION

To realize the promise of nuclear fusion and make it an economical energy source, tokamak reactors must operate for long periods of time in a burning plasma mode characterized by a high Q, where Q is the ratio of fusion power to auxiliary power. Although stable operating points with this characteristic exist for most confinement scalings, they are usually found in a region of high temperature and low density. It is possible, however, that economic and technological constraints will require future commercial fusion reactors to run at low temperature and high density operating points in which the rate of thermonuclear reaction increases as the plasma temperature rises. Under these conditions, an active control system may be necessary to stably control the plasma density and temperature and prevent small perturbations in temperature or density from growing. Small increases in temperature may cause thermal excursions in which the system moves to a new, stable equilibrium at a higher temperature, or, in the case of decreases in temperature, the loss of heating power could lead to quenching. In either case, disruptive plasma instabilities could be triggered, stopping operation and possibly causing wall damage.

Over the years, the physical and technological feasibility of different methods for controlling the burn condition have been studied. Prior work, including [1], [2], [3], considered modulation of auxiliary power, modulation of fueling rate, and injection of impurities as actuators. Most existing burn control efforts use only one of the available actuators (single-input control) and linearize the system model to make use of linear control techniques. When tested using nonlinear models, these controllers succeed in stabilizing the system against a limited set of perturbations. In [4], a diagonal multi-input, multi-output control scheme was developed for controlling burning plasma kinetics, though the authors point out that due to the complexity of the plasma system, nonlinear control is needed for the most economic and reliable modes of operation. In our previous work [5], a zero-dimensional nonlinear model involving approximate conservation equations for the energy and the densities of the species was used to synthesize a nonlinear feedback controller for stabilizing the burn condition of a fusion reactor. The controller makes use of all of the previously considered actuators simultaneously, using auxiliary power modulation to prevent quenching, impurity injection to increase radiation losses and stop thermal excursions, and fueling modulation to stabilize the density. The use of nonlinear control techniques removes the operability limits imposed by linearization in other works. A 0-D computer simulation study was performed to show the capability of the controller and compare it with previous linear controllers. Nonlinear control using multiple actuators had only been done previously in works using non-model based techniques, like neural networks [6], [7].

The nonlinear controller designed in our work [5] guarantees a much larger region of attraction than the previous linear controllers. However, the control scheme requires impurity injection to reject thermal excursions, which could lead to undesirable accumulation of impurity ions within the plasma core. Also, the model used for design assumed an optimal 50:50 mix of deuterium and tritium within the plasma at all times. Because experiments indicate that deuterium and tritium may have different transport properties [8], the deuterium and tritium systems should be actuated separately to allow for control of the isotopic mix in the core. Such a scheme should be possible in ITER, based on the proposed fueling system, which is to include both pellet and gas injection systems, and the available diagnostics. The pellet injection system will include two pellet injectors - one for pellets of primarily deuterium and the other for

This work was supported by the NSF CAREER award program (ECCS-0645086). M. D. Boyer (mdb209@lehigh.edu), and E. Schuster are with the Department of Mechanical Engineering and Mechanics, Lehigh University, Bethlehem, PA 18015, USA.

pellets of primarily tritium. The gas injection system will be used to supply deuterium at the edge of the plasma. Together, these systems will allow the fuel mix to be altered in a technique called isotopic fuel tailoring [9]. The ratio of tritium to deuterium within the plasma is important for reactor operation and burn control, as well as safety and commissioning of devices. First, because the fusion power is a maximum with a 50:50 DT mix, the mix should be kept near 50:50 during steady state operation. Secondly, because tritium levels in the plasma facing parts of the machine depend directly on the relative amount of tritium in the plasma's edge, the machine could be made safer and easier to commission if the amount of tritium in the plasma's edge is kept low [10]. Lastly, as we will show in this work, it is possible to exploit the reduction in fusion power caused by modulating the relative mix of DT fuel as a way to stabilize thermal excursions without the need for impurity injection.

The controller presented here is designed to stabilize the volume averaged densities of alpha-particles, deuterium ions, and tritium ions, as well as the volume averaged energy density. The controller can deal with perturbations in initial conditions leading to either thermal excursion or quenching, and its effectiveness is independent of whether the operating point is an ignition (no auxiliary heating) or subignition point. The nonlinear controller depends parametrically on the equilibrium, allowing it to drive the system from one equilibrium point to another. This will be essential for modulating power and other plasma parameters during reactor operation. Simulation results show successful stabilization of the desired equilibrium.

The paper is organized as follows. In Section II a zero-dimensional model of the dynamics is introduced. The control objective is stated in Section III. The design of a nonlinear stabilizing controller is presented in Section IV. Simulation parameters and results, showing both the open loop and closed loop response of the system, are presented in Section V. Finally, conclusions and plans for future work are stated in Section VI.

II. Burning Plasma Model

In this work we use a zero-dimensional model for a burning plasma which employs approximate energy and particle balance equations. The model is fundamentally the same as that used in [11], and also [5]. However, unlike the model used in these previous pieces of work, the model considered here treats the deuterium and tritium ion densities separately, which allows us to make use of isotopic fuel tailoring as an additional actuator. The model is given by

$$\frac{dn_\alpha}{dt} = -\frac{n_\alpha}{\tau_\alpha} + n_D n_T \langle\sigma v\rangle \quad (1)$$

$$\frac{dn_D}{dt} = -\frac{n_D}{\tau_D} - n_D n_T \langle\sigma v\rangle + S_D \quad (2)$$

$$\frac{dn_T}{dt} = -\frac{n_T}{\tau_T} - n_D n_T \langle\sigma v\rangle + S_T \quad (3)$$

$$\frac{dE}{dt} = -\frac{E}{\tau_E} + Q_\alpha n_D n_T \langle\sigma v\rangle - P_{rad} + P_{aux} \quad (4)$$

where n_α, n_D, and n_T are the alpha-particle, deuterium, and tritium densities, respectively, and E is the energy. Parameters τ_α, τ_D, τ_T, τ_E are the alpha-particle, deuterium, tritium, and energy confinement times, respectively. The control inputs are the deuterium and tritium fueling rates, given by S_D and S_T, as well as the auxiliary heating, P_{aux}. This approximate model implies that the alpha-particles slow down instantaneously and deposit their energy ($Q_\alpha = 3.52$ MeV) in the flux surface in which they are born, which is a reasonable approximation for reactor-size tokamaks.

The DT reactivity $\langle\sigma v\rangle$ is a highly nonlinear, positive, and bounded function of the plasma temperature T and is calculated by

$$\langle\sigma v\rangle = exp\left(\frac{a_1}{T^r} + a_2 + a_3 T + a_4 T^2 + a_5 T^3 + a_6 T^4\right) \quad (5)$$

where the parameters a_i and r are taken from [12]. In this work, the radiation loss P_{rad} is approximated as

$$P_{rad} = P_{brem} = A_b Z_{eff} n_e^2 \sqrt{T} \quad (6)$$

where $A_b = 5.5\times10^{-37}$ $\mathrm{Wm^3/\sqrt{keV}}$ is the bremsstrahlung radiation coefficient, Z_{eff} is the effective atomic number, and n_e is the electron density. No explicit evolution equation is provided for the electron density as it is obtained from the neutrality condition $n_e = n_D + n_T + 2n_\alpha$. The effective atomic number, plasma density, and temperature are given by

$$Z_{eff} = \sum_i \frac{n_i Z_i^2}{n_e} = \frac{n_D + n_T + 4n_\alpha}{n_e} \quad (7)$$

$$n = n_\alpha + n_D + n_T + n_e = 2n_D + 2n_T + 3n_\alpha \quad (8)$$

$$T = \frac{2}{3}\frac{E}{n} \quad (9)$$

where Z_i is the atomic number of the different ions. The energy confinement time scaling used in this work is ITER90H-P [13] because it allows for performance comparison with previous work, however, this choice only affects the simulation study. The controller design is independent of the scaling used. The scaling used is

$$\tau_E = f0.082 I^{1.02} R^{1.6} B^{0.15} A_i^{0.5} \kappa_\chi^{-0.19} P^{-0.47} = fkA_i^{0.5} P^{-0.47} \quad (10)$$

The factor scale f depends on the confinement mode and is determined by comparing the net plasma heating power P to the L-H transition power. For the simulations in this work, the system remains in H-mode, for which we use $f = 0.85$. Parameters I, R, B, κ_χ, are assumed to be kept constant by a magnetic controller, such that they can be collapsed into a single constant, k. The isotopic number A_i is given by

$$A_i = 3\gamma + 2(1-\gamma) = \gamma + 2 \quad (11)$$

with γ being the tritium fraction. This is the fraction of hydrogen that is tritium and can be expressed as

$$\gamma = n_T/(n_D + n_T) \quad (12)$$

The net plasma heating power P is defined as

$$P = P_{fusion} - P_{rad} + P_{aux} \quad (13)$$

The fusion power is given by

$$P_{fusion} = Q_\alpha n_D n_T \langle\sigma v\rangle = Q_\alpha \gamma(1-\gamma) n_H^2 \langle\sigma v\rangle \quad (14)$$

TABLE I

REACTOR PARAMETERS

I	Plasma current	22.0 MA
R	Major radius	6.0 m
a	Minor radius	2.15 m
B	Magnetic Field	4.85 T
κ_χ	Elongation at χ	2.2
k_α	Alpha-particle confinement constant	7
k_D	Deuterium particle confinement constant	3.6
k_T	Tritium particle confinement constant	2.6
β_{max}	Beta limit	2.5I/aB=5.3%
V	Plasma volume	1100 m^3

where $n_H = n_D + n_T$ is the total hydrogen density. Note the parabolic relationship between fusion power and tritium fraction γ, which will be exploited for controlling thermal excursions.

The confinement times for the different species are scaled with the energy confinement time τ_E as

$$\tau_\alpha = k_\alpha \tau_E,\ \tau_D = k_D \tau_E,\ \tau_T = k_T \tau_E \tag{15}$$

Reactor parameters used in this work are given in Table I.

III. CONTROL OBJECTIVE

The possible steady-state operating points of the reactor are given by the equilibria of the dynamic equations. The equilibrium values of the energy $\bar{E}$, the density variables $\bar{n}_\alpha$, $\bar{n}_D$, $\bar{n}_T$, the fueling source terms $\bar{S}_D$, $\bar{S}_T$, and the auxiliary heating $\bar{P}_{aux}$, are determined by solving the nonlinear algebraic equations obtained by setting the left side of Eqs. (1) through (4) to zero when two of the plasma parameters, such as T and plasma β[1], for example, are chosen arbitrarily i.e.

$$0 = -\frac{\bar{n}_\alpha}{\bar{\tau}_\alpha} + \bar{n}_D \bar{n}_T \langle \bar{\sigma v} \rangle \tag{16}$$

$$0 = -\frac{\bar{n}_D}{\bar{\tau}_D} - \bar{n}_D \bar{n}_T \langle \bar{\sigma v} \rangle + \bar{S}_D \tag{17}$$

$$0 = -\frac{\bar{n}_T}{\bar{\tau}_T} - \bar{n}_D \bar{n}_T \langle \bar{\sigma v} \rangle + \bar{S}_T \tag{18}$$

$$0 = -\frac{\bar{E}}{\bar{\tau}_E} + Q_\alpha \bar{n}_D \bar{n}_T \langle \bar{\sigma v} \rangle - \bar{P}_{rad} + \bar{P}_{aux} \tag{19}$$

In this work, we only consider equilibria with the optimal tritium ratio $\gamma = 0.5$. By defining the deviations from the equilibrium values as $\tilde{n}_\alpha = n_\alpha - \bar{n}_\alpha$, $\tilde{n}_D = n_D - \bar{n}_D$, $\tilde{n}_T = n_T - \bar{n}_T$, and $\tilde{E} = E - \bar{E}$, the dynamic equations for the deviations can be written as

$$\frac{d\tilde{n}_\alpha}{dt} = -\frac{\tilde{n}_\alpha}{\tau_\alpha} - \frac{\bar{n}_\alpha}{\tau_\alpha} + S_\alpha \tag{20}$$

$$\frac{d\tilde{n}_D}{dt} = -\frac{\tilde{n}_D}{\tau_D} - \frac{\bar{n}_D}{\tau_D} - S_\alpha + S_D \tag{21}$$

$$\frac{d\tilde{n}_T}{dt} = -\frac{\tilde{n}_T}{\tau_T} - \frac{\bar{n}_T}{\tau_T} - S_\alpha + S_T \tag{22}$$

$$\frac{d\tilde{E}}{dt} = -\frac{\tilde{E}}{\tau_E} - \frac{\bar{E}}{\tau_E} + Q_\alpha S_\alpha - P_{rad} + P_{aux} \tag{23}$$

where the nonlinear alpha-particle source term is written as

$$S_\alpha(E, n_D, n_T, n_\alpha) = n_D n_T \langle \sigma v \rangle = \gamma(1-\gamma) n_H^2 \langle \sigma v \rangle \tag{24}$$

[1]The plasma β is the ratio of plasma pressure to magnetic pressure and is given by $\beta = \frac{knT}{(B^2/2\mu_0)}$ where B is the magnetic field strength, μ_0 is the permeability of free space, and k is the Boltzmann constant.

to simplify the presentation. Recall from (5) and (9) that $\langle \sigma v \rangle$ is a function of E, n_D, n_T, and n_α. The objective of the control law is to force the initial perturbations $\tilde{n}_\alpha$, $\tilde{n}_D$, $\tilde{n}_T$, $\tilde{E}$ to zero by modulation of the fuel sources S_D, S_T, as well as the auxiliary power P_{aux}. It is assumed that all states are available from either measurement or estimation. P_{aux} is used to stabilize the energy system during negative perturbations, however, P_{aux} cannot be reduced below zero, so large positive perturbations in temperature require the use of another actuator. In previous work, controlled injection of impurities was used to increase radiation losses and stabilize such excursions. In this work, we avoid the use of impurities by utilizing the ITER fueling system's ability to perform isotopic fuel tailoring. For this initial work, we assume ideal actuators. In future work, it will be necessary to account for actuator dynamics.

IV. CONTROLLER DESIGN

The design begins by looking for a control which stabilizes $\tilde{E}$. If the condition

$$Q_\alpha S_\alpha - P_{rad} + P_{aux} = \frac{\bar{E}}{\tau_E} \tag{25}$$

is satisfied, equation (23) is reduced to

$$\frac{d\tilde{E}}{dt} = -\frac{\tilde{E}}{\tau_E} \tag{26}$$

and the $\tilde{E}$ subsystem is then exponentially stable since $\tau_E > 0$. Condition (25) is met by modulating the alpha-heating term $Q_\alpha S_\alpha$ and the auxiliary heating P_{aux}. Modulation of the alpha-heating term is done through altering the tritium fraction $\gamma = n_T/(n_D + n_T)$ within the plasma. The stabilizing controller is calculated as follows:

First Step: We first set $P_{aux} = 0$ and seek a tritium fraction $\gamma = \gamma^*$ that satisfies condition (25). Writing the alpha-particle generation term S_α in terms of γ^*, condition (25) becomes

$$Q_\alpha \gamma^*(1-\gamma^*) n_H^2 \langle \sigma v \rangle - P_{rad} = \frac{\bar{E}}{\tau_E} \tag{27}$$

This equation can be solved for γ^*, yielding

$$\gamma^*(1-\gamma^*) = \frac{\frac{\bar{E}}{\tau_E} + P_{rad}}{Q_\alpha n_H^2 \langle \sigma v \rangle} = C \tag{28}$$

$$\gamma^* = \frac{1 \pm \sqrt{1-4C}}{2} \tag{29}$$

If $C \leq 0.25$, the two resulting solutions for γ^* are real. Because economic and safety considerations make it undesirable to use more tritium than necessary in a reactor, we take only the solution satisfying $\gamma^* \leq 0.5$. If $C \geq 0.25$, there is no real value of γ^* that satisfies condition (25), so we set $\gamma^* = 0.5$, and move on to the second step.

Second Step: If $\gamma^* = 0.5$, the condition (25) cannot be met by altering the tritium ratio alone and additional heating is needed. In this case, we calculate the auxiliary power as

$$P_{aux} = \frac{\bar{E}}{\tau_E} - Q_\alpha \gamma^*(1-\gamma^*) n_H^2 \langle \sigma v \rangle + P_{rad} \tag{30}$$

Based on the control objectives and the previous steps, we now have desired reference values for the energy, $\bar{E}$, the tritium fraction, γ^*, and the hydrogen density, $\bar{n}_H = \bar{n}_D + \bar{n}_T$. We next stabilize these references with the fueling terms S_D and S_T. We begin by defining $\hat{\gamma} = \gamma - \gamma^*$ and

$$f(\gamma, \tilde{E}, \tilde{n}_\alpha, \tilde{n}_D, \tilde{n}_T) = -\frac{\bar{E}}{\tau_E} + Q_\alpha S_\alpha - P_{rad} + P_{aux} \quad (31)$$

$$f(\gamma^*, \tilde{E}, \tilde{n}_\alpha, \tilde{n}_D, \tilde{n}_T) = 0 \quad (32)$$

where the last relation is a consequence of our choice of γ^* and P_{aux} in (29) and (30). The last relation allows us to write $f = \hat{\gamma}\phi$, where ϕ is a continuous function. This allows us to rewrite (23) as

$$\frac{d\tilde{E}}{dt} = -\frac{\tilde{E}}{\tau_E} + \hat{\gamma}\phi \quad (33)$$

Recalling the definition of the tritium ratio, $\gamma = n_T/n_H$, we can write the equation governing its dynamics as

$$\dot{\gamma} = \dot{\hat{\gamma}} + \dot{\gamma}^* = \frac{\dot{n}_T n_H - n_T \dot{n}_H}{n_H^2} = \frac{\dot{n}_T}{n_H} - \gamma\frac{\dot{n}_H}{n_H} \quad (34)$$

$$\dot{\hat{\gamma}} = \frac{1}{n_H}\left[\dot{n}_T - \gamma\dot{n}_H\right] - \dot{\gamma}^* \quad (35)$$

We recall (21) and (22) to write

$$\dot{n}_T = \dot{\tilde{n}}_T = -\frac{n_T}{\tau_T} - S_\alpha + S_T \quad (36)$$

$$\dot{n}_H = \dot{\tilde{n}}_H = \dot{\tilde{n}}_T + \dot{\tilde{n}}_D = -\frac{n_T}{\tau_T} - \frac{n_D}{\tau_D} - 2S_\alpha + S_D + S_T \quad (37)$$

$$\begin{aligned}\dot{\hat{\gamma}} =& \frac{1}{n_H}\left[-\frac{n_T}{\tau_T} - S_\alpha + S_T - n_H\dot{\gamma}^*\right.\\ &\left.-\gamma\left(-\frac{n_T}{\tau_T} - \frac{n_D}{\tau_D} - 2S_\alpha + S_D + S_T\right)\right]\end{aligned} \quad (38)$$

Now that the necessary dynamic equations are available, we take the Lyapunov function candidate

$$V = \frac{k_1^2\tilde{E}^2 + k_2^2\hat{\gamma}^2 + \tilde{n}_H^2}{2} \quad (39)$$

where $k_1 = 10^{15}$ and $k_2 = 10^{20}$ (recall that $\tilde{E} = O(10^5)$, $\hat{\gamma} = O(10^{-1})$, and $\tilde{n}_H = O(10^{20})$) and compute

$$\dot{V} = k_1^2\tilde{E}\dot{\tilde{E}} + k_2^2\hat{\gamma}\dot{\hat{\gamma}} + \tilde{n}_H\dot{\tilde{n}}_H \quad (40)$$

$$\begin{aligned}=& -\frac{k_1^2\tilde{E}^2}{\tau_E} + k_1^2\tilde{E}\hat{\gamma}\phi + \frac{k_2^2\hat{\gamma}}{n_H}\left[-\frac{n_T}{\tau_T} - S_\alpha + S_T - n_H\dot{\gamma}^*\right.\\ &\left.-\gamma\left(-\frac{n_T}{\tau_T} - \frac{n_D}{\tau_D} - 2S_\alpha + S_D + S_T\right)\right]\\ &+\tilde{n}_H\left[-\frac{n_T}{\tau_T} - \frac{n_D}{\tau_D} - 2S_\alpha + S_D + S_T\right]\end{aligned} \quad (41)$$

$$\begin{aligned}=& -\frac{k_1^2\tilde{E}^2}{\tau_E} + \frac{k_2^2\hat{\gamma}}{n_H}\left[\frac{k_1^2 n_H\tilde{E}\phi}{k_2^2} - \frac{n_T}{\tau_T} - S_\alpha + S_T - n_H\dot{\gamma}^*\right.\\ &\left.-\gamma\left(-\frac{n_T}{\tau_T} - \frac{n_D}{\tau_D} - 2S_\alpha + S_D + S_T\right)\right]\\ &+\tilde{n}_H\left[-\frac{n_T}{\tau_T} - \frac{n_D}{\tau_D} - 2S_\alpha + S_D + S_T\right]\end{aligned} \quad (42)$$

We begin by stabilizing the part of (42) relating to the dynamics of $\tilde{n}_H$ by taking

$$S_D = \frac{n_T}{\tau_T} + \frac{n_D}{\tau_D} + 2S_\alpha - S_T - K_D\tilde{n}_H \quad (43)$$

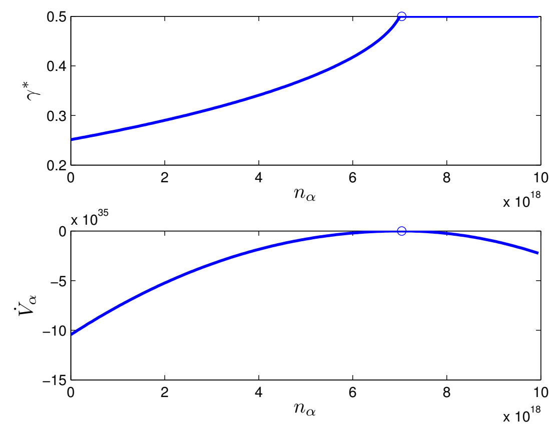

Fig. 1. Top: Values of γ^* for a range of values of n_α. Bottom: Values of $\dot{V}_\alpha$ for a range of values of n_α. The circle denotes the desired equilibrium.

where $K_D > 0$. This reduces equation (42) to

$$\begin{aligned}\dot{V} =& \frac{k_2^2\hat{\gamma}}{n_H}\left[\frac{k_1^2 n_H\tilde{E}\phi}{k_2^2} - \frac{n_T}{\tau_T} - S_\alpha + S_T - n_H\dot{\gamma}^* + \gamma K_D\tilde{n}_H\right]\\ &-\frac{k_1^2\tilde{E}^2}{\tau_E} - K_D\tilde{n}_H^2\end{aligned} \quad (44)$$

Finally, we take

$$S_T = -\frac{k_1^2 n_H\tilde{E}\phi}{k_2^2} + \frac{n_T}{\tau_T} + S_\alpha + n_H\dot{\gamma}^* - \gamma K_D\tilde{n}_H - K_T\hat{\gamma} \quad (45)$$

such that S_D becomes

$$S_D = \frac{n_D}{\tau_D} + S_\alpha + \frac{k_1^2 n_H\tilde{E}\phi}{k_2^2} - n_H\dot{\gamma}^* - (1-\gamma)K_D\tilde{n}_H + K_T\hat{\gamma} \quad (46)$$

and equation (44) is reduced to

$$\dot{V} = -\frac{k_1^2\tilde{E}^2}{\tau_E} - K_D\tilde{n}_H^2 - \frac{K_T k_2^2\hat{\gamma}^2}{n_H} \quad (47)$$

such that $\dot{V} < 0$ when the deviation variables are nonzero. This guarantees that the energy and hydrogen density subsystems are stabilized, and that the tritium fraction γ converges to γ^*. By making $\gamma = \gamma^*$ and choosing the necessary value of P_{aux}, the controller guarantees that the system satisfies condition (25). Once $n_H = \bar{n}_H$ and $E = \bar{E}$, we note that T, n_e, Z_{eff}, and therefore P_{rad}, are only functions of n_α. The reactivity, being a function of T, is also only a function of n_α. The fusion power (14) is then only a function of n_α and γ. Thus, for any given perturbation in n_α, we can find the value of $\gamma = \gamma^*$ that would satisfy condition (25). For the equilibrium given in Table II, the value of γ^* at a range of values of n_α is shown in the top plot of Figure 1. Each value of n_α and γ^*, can then be used to calculate the terms in the dynamic equation for $\tilde{n}_\alpha$, equation (20). We then take the Lyapunov function $V_\alpha = \frac{1}{2}\tilde{n}_\alpha^2$ and calculate for each value of n_α the quantity $\dot{V}_\alpha = \tilde{n}_\alpha\dot{\tilde{n}}_\alpha$. In the bottom plot of Figure 1, we see that for the equilibrium given in Table II, $\dot{V}_\alpha < 0$ at all physically significant values of n_α. This shows that the controller stabilizes the n_α system against any perturbation. A similar study could be done for other equilibrium points.

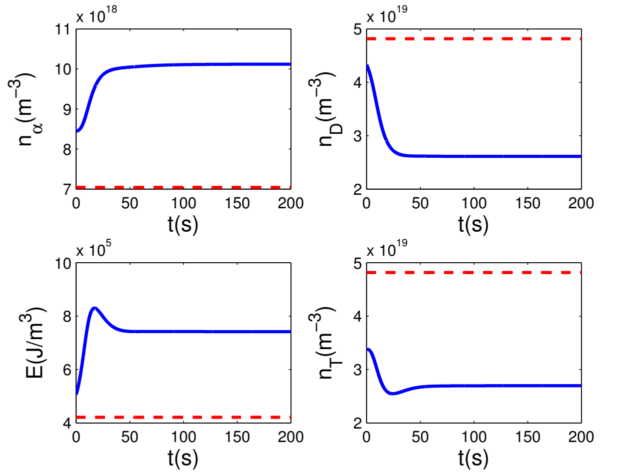

Fig. 2. Evolution of open loop states (blue-solid) compared with equilibrium values (red-dashed).

Once $n_\alpha = \bar{n}_\alpha$, we see from Figure 1 that we must have $\gamma^* = .5$, the equilibrium value of γ. Recalling that n_H goes to $\bar{n}_H$, this guarantees that n_D and n_T are stabilized. We now have that the states E, n_D, n_T, and n_α are stabilized by the control laws given by equations (30), (45), and (46).

V. Simulation Results

In this section we show the performance of the controller for the equilibrium point characterized by the values given in Table II. The simulations shown were all done using the initial perturbations $n_H(0) = 0.80\bar{n}_H$, $\gamma(0) = 0.88\bar{\gamma}$, $n_\alpha(0) = 1.20\bar{n}_\alpha$, and $E(0) = 1.20\bar{E}$.

In the open loop simulation, the system is initially perturbed and the actuators are kept constant at their equilibrium values. The simulation shows that without active control, a thermal excursion occurs and the system moves away from the desired equilibrium. Figure 2 shows the evolution of the states. Note that the hydrogen density drops, the energy increases sharply, and the α-particle density rises with the increased reactivity. This is reflected in Figure 3, which shows the temperature, density, and β.

In the closed loop simulation, the controller alters the fueling and heating in order to force the system to the desired equilibrium. Figure 4 shows the evolution of the average ion densities and energy during the closed loop simulation while Figure 5 depicts the evolution of the temperature, density and β. After a thermal excursion, the states are all successfully returned to their desired equilibrium values. Figure 6 shows the time history of the actuators in closed loop. The plot

TABLE II

Equilibrium Point

$\bar{T}$	Temperature	8.2 keV
$\bar{\beta}$	Plasma Beta	3%
$\bar{n}$	Plasma Density	2.14×10^{20} m^{-3}
$\bar{n}_H$	Hydrogen Density	9.63×10^{19} m^{-3}
$\bar{\gamma}$	Tritium Fraction	0.5
$\bar{n}_\alpha$	Alpha-particle Density	7.04×10^{18} m^{-3}
$\bar{E}$	Energy Density	4.21×10^5 J/m^3
$\bar{S}_D$	Deuterium Fueling Rate	2.11×10^{18} m^{-3} s^{-1}
$\bar{S}_T$	Tritium Fueling Rate	2.87×10^{18} m^{-3} s^{-1}
$\bar{P}_{aux}$	Auxiliary Power	168 W/m^3

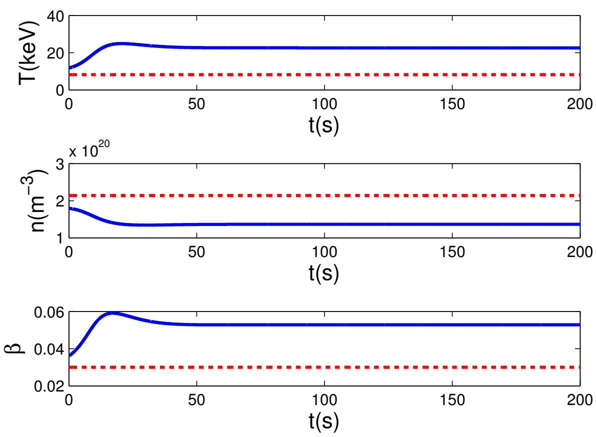

Fig. 3. Evolution of open loop T, n, and β (blue-solid) compared with equilibrium values (red-dashed).

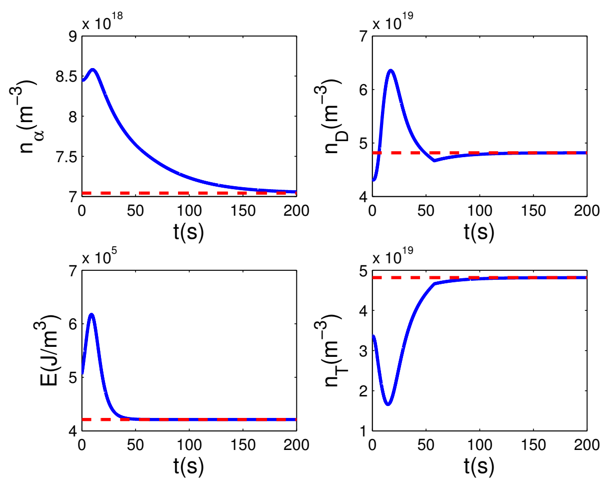

Fig. 4. Evolution of closed loop states (blue-solid) compared with equilibrium values (red-dashed).

shows how the fuel injection rates and the auxiliary power work in tandem to control the energy of the system. Note that ramp rate limits have been imposed on the actuators during the simulation. The top plot of Figure 7 shows the time evolution of γ and γ^*. Finally, the bottom plot of Figure 7 shows the time evolution of the plasma heating power P. Note that once $\gamma = \gamma^* = .5$ the power goes to its equilibrium value, as the only solution to (25) is $P = \bar{P}$.

VI. Conclusions and Future Work

We have presented a nonlinear burn stability controller capable of rejecting perturbations in the ion species densities and energy, returning the subsystems to their desired values. By avoiding linearization, the controller can deal with a larger set of perturbations than previous linear controllers and the multi-input scheme allows it to reject perturbations leading to both thermal excursion and quenching. In addition, the effectiveness of the controller does not depend on whether the operating point is an ignition or subignition point.

The DT ion densities are handled separately, allowing for control of the DT fuel mix, which is exploited to control thermal excursions. This scheme avoids the need for impurity injection into the plasma core. The system was simulated

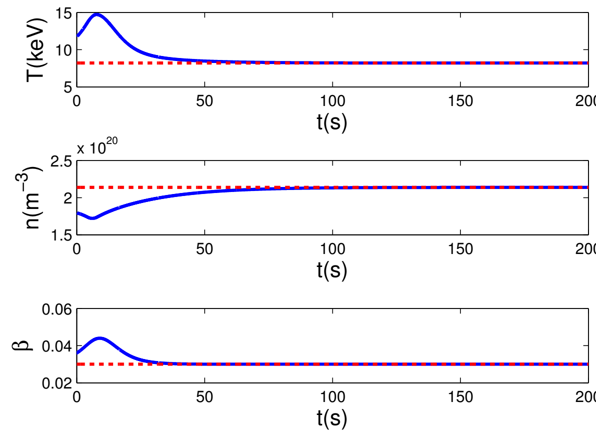

Fig. 5. Evolution of closed loop T, n, and β (blue-solid) compared with equilibrium values (red-dashed).

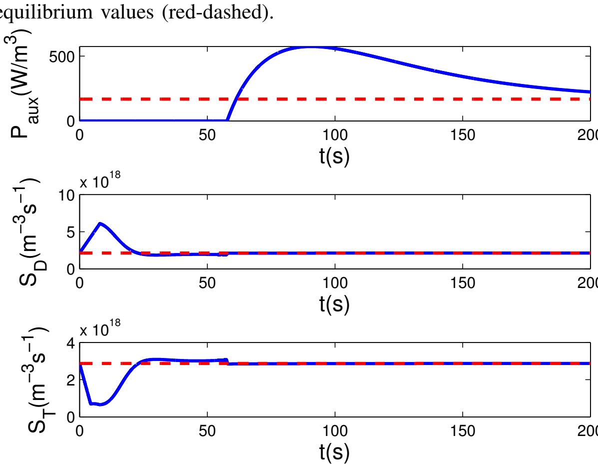

Fig. 6. Actuation (blue-solid) compared to equilibrium values (red-dotted).

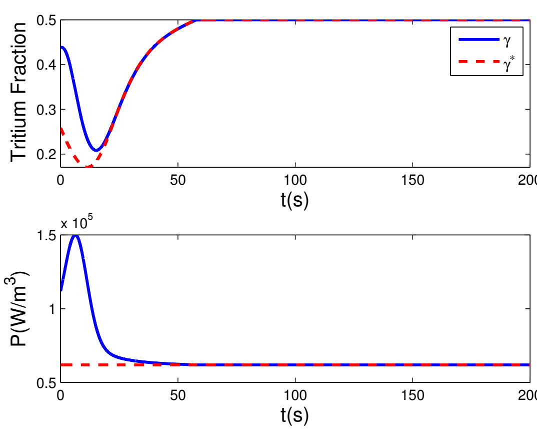

Fig. 7. Top: Tritium ratio, γ, compared to the value called for by the controller, γ^*. Bottom: Plasma heating P (blue-solid) compared with the equilibrium value of plasma heating $\bar{P}$ (red-dashed).

in open and closed loop to show the need for and the effectiveness of the proposed controller. The simulations show that for a given set of initial conditions the open loop response of the system is unstable and that the controller forces the system back to the desired equilibrium.

Since the nonlinear controller depends parametrically on the equilibrium, it can drive the system from one working point to another, allowing for changes in power and other parameters without the need for scheduled controllers.

It should be noted that this approach could be used for any confinement time scalings (10) and is not restricted to the ITER scaling used here. It should also be noted that the expressions for confinement used here were derived by experiment and that these experiments are usually done under time-stationary states. Thus, it is unclear whether the empirical confinement time can be safely applied. For larger excursions from equilibrium (i.e., when $(1/\tilde{E})(d\tilde{E}/dt > 1/\tau_E)$ the empirical expression for τ_E may break down. In this case, an alternate expression should be used, or a one-dimensional model could be used to incorporate plasma profile evolution information during transients.

Uncertainty and variation in the confinement time scaling (15), as well as variation in reaction rate and radiation losses from the one-dimensional kinetic profile shapes, should be considered. Available control tools for dealing with uncertainties will be considered. Another approach will be to modify the nonlinear control design to use available kinetic profile measurements. Both approaches will be studied with a one-dimensional burning plasma model and will be a step towards kinetic profile control in burning plasmas, an issue with implications for other fusion control problems, like transport control, confinement improvement, and MHD stability. The long-term goal is to design model-based controllers for simultaneous kinetic profile regulation and burn condition control combining all available actuation methods, including boundary (gas-puffing) and interior (pellet injection, auxiliary heating) actuators.

References

[1] J. Mandrekas and W. M. Stacey, "Evaluation of Different Burn Control Methods for the International Thermonuclear Experimental Reactor," *13th IEEE Symp. on Fusion Eng.*, vol. 1, pp. 404–407, 1989.

[2] S. Haney, L. J. Perkins, J. Mandrekas, and W. M. Stacey, "Active Control of Burn Conditions for the International Thermonuclear Experimental Reactor," *Fusion Tech.*, vol. 18, no. 4, pp. 606–17, 1990.

[3] D. Anderson, T. Elevant, H. Hamen, M. Lisak, and H. Persson, "Studies of Fusion Burn Control," *Fusion Tech.*, vol. 23, no. 1, pp. 5–41, 1993.

[4] V. M. Leonov, Y. V. Mitrishkin, and V. E. Zhogolev, "Simulation of burning ITER plasma in multi-variable kinetic control system," in *32nd EPS Conf. on Plasma Phys.*, vol. 29, no. July, 2005, pp. 2–5.

[5] E. Schuster and M. Krstic, "Burn Control in Fusion Reactors via Nonlinear Stabilization Techniques," *Fusion Sci. and Tech.*, vol. 43, 2003.

[6] J. Vitela, "Burn conditions stabilization with artificial neural networks of subignited thermonuclear reactors with scaling law uncertainties," *Plasma Phys. Control. Fusion*, vol. 43, pp. 99–119, 2001.

[7] ——, "Stabilization of burn conditions in a thermonuclear reactor using artificial neural networks," *Plasma Phys. Control. Fusion*, vol. 40, pp. 295–318, 1998.

[8] K.-D. Zastrow, J. M. Adams, Y. Baranov, P. Belo, L. Bertalot *et al.*, "Tritium transport experiments on the JET tokamak," *Plasma Phys. Control. Fusion*, vol. 46, no. 12B, pp. B255–B265, Dec. 2004.

[9] L. Baylor, P. Parks, T. Jernigan, J. Caughman, S. Combs, C. Foust, W. A. Houlberg, S. Maruyama, and D. Rasmussen, "Pellet fuelling and control of burning plasmas in ITER," *Nucl. Fusion*, vol. 47, pp. 443–448, 2007.

[10] M. Gouge, W. A. Houlberg, S. Attenberger, and S. Milora, "Fuel Source Isotopic Tailoring and Its Impact on ITER Design, Operation and Safety," *Fusion Technol.*, pp. 1–18, 1995.

[11] W. Hui, K. Fischbach, B. Bamieh, and G. Miley, "Effectiveness and constraints of using the refueling system to control fusion reactor burn," *15th IEEE/NPSS Symp. on Fusion Eng*, pp. 562–564, 1993.

[12] L. Hively, "Special Topic Convenient Computational Forms For Maxwellian Reactivities," *Nucl. Fusion*, 1977.

[13] N. Uckan, "ITER Physics Design Guidelines: 1989," *ITER Documentation Series No. 10, International Atomic Energy Agency*, 1990.